



Research Article

Effect of baffle angles on flow and heat transfer in a circular duct with nanofluids

Selma Akçay ^{a,*}  and Unal Akdag ^b 

^aMechanical Engineering Department, Çankırı Karatekin University, Çankırı, 18100, Turkey

^bMechanical Engineering Department, Aksaray University, Aksaray, 68100, Turkey

ARTICLE INFO

Article history:

Received 27 June 2022

Accepted 01 October 2022

Published 15 December 2022

Keywords:

Baffle
Friction factor
Heat transfer
Nanofluid

ABSTRACT

This work numerically analyzes the hydraulic and thermal performance of CuO-water nanofluid in a circular duct with different baffle angles. In the numerical work, governing equations are discretized with the finite volume method, and the simulations are solved with SIMPLE algorithm. The surfaces of the duct containing baffles are kept at 340 K. In the analysis, the effects of different Reynolds numbers ($200 \leq Re \leq 1000$), nanoparticle volume fractions ($1\% \leq \phi \leq 3\%$), and baffle angles ($30^\circ \leq \alpha \leq 150^\circ$) on the thermal enhancement factor (η) and the friction factor are investigated. In addition, the flow and temperature contours are presented for different parameters within the duct. From those contours, it is observed that the baffles cause flow oscillation and recirculation zones are formed. The numerical results show that baffles and nanofluid flow contribute significantly to the thermal enhancement. The Nusselt number (Nu) and relative friction factor (r) increase as the Reynolds number and nanoparticle volume fraction increase. While the highest thermal enhancement factor and relative friction factor are obtained at $\alpha = 90^\circ$ baffle angle, the best performance evaluation criterion (PEC) value is found at $\alpha = 150^\circ$ baffle angle.

1. Introduction

Heat transfer improvement is an important research topic in many engineering fields. Passive methods used to increase the heat transfer of thermal devices provide significant advantages and cost savings. These methods include the applications such as baffles, twisted tapes, wire coil inserts, swirl generators, and the use of wavy/ribbed surfaces. Passive methods may have simplicity and require less or no additional system components, but they increase pressure drop significantly. These methods are preferred in various fields such as solar air ducts, heating/cooling applications, heat exchangers, cooling processing of gas turbine blade, nuclear reactors, transportation, food and chemical industry, etc. [1-4]. Flow and heat transfer in wavy channels have been examined theoretically and experimentally by many researchers and it was reported that the wavy surface geometry has an important potential on the heat transfer improvement due to both increasing the surface area and providing fluctuation in flow. However, it was declared these surfaces rise the pressure loss compared to straight ducts [5-7]. For this, flat ducts with relatively less pressure drop are preferred and it is

aimed to increase the thermal performance with the baffles added to the duct surfaces. It was reported that the baffles, which act similar to turbulators, increase heat transfer by improving flow mixing [8-15].

Menni et al. [16] numerically examined the flow and thermal performance of solar air ducts with different baffles. Menni et al. [17] examined the aerodynamic and thermal properties of multiple V fins in solar air ducts. In their work was changed in the fin attack-angle, length, and separation length, at different the flow rate. They reported that an optimum thermal enhancement factor was yielded for a 40° attack angle at $Re = 2163$. Salhi et al. [18] theoretically studied the effects of longitudinal baffles on hydraulic and thermal performance in tubular heat exchangers. In another study, Salhi et al. [19] analyzed the heat and mass transfer of partially inclined baffles in different arrangements in a straight duct for turbulent air flow. The results indicated that the thermal performance improved by 32.37% for the triangular baffles, and by 44.37% for the rectangular baffles. Nedunchezhiyan et al. [20] conducted a theoretic work examining the effects of baffles on flow and heat transfer. Razavi et al. [21] examined the effects on hydraulic and thermal improvement of the inclination angle of perforated

* Corresponding author. Tel.: +90-376-218-9532; Fax: +90-376-218-9536.

E-mail addresses: selmaakçay@karatekin.edu.tr (S. Akçay), uakdag@aksaray.edu.tr (U. Akdag)

ORCID: 0000-0003-2654-0702 (S. Akçay), 0000-0002-1149-7425 (U. Akdag)

DOI: [10.35860/iaiej.1136354](https://doi.org/10.35860/iaiej.1136354)

© 2022, The Author(s). This article is licensed under the CC BY-NC 4.0 International License (<https://creativecommons.org/licenses/by-nc/4.0/>).

baffles in a rectangular channel under laminar flow conditions. Al Habet et al. [22] analyzed the thermal and hydraulic performance of perforated baffles in an inline and staggered arrangement in a rectangular duct. These studies indicated that thermal and hydraulic behaviors changed depending on the flow structure, channel geometry, baffle shape, baffle arrangement, and baffle angle.

Manca et al. [23] analyzed the thermal improvement of Al_2O_3 -water nanofluid for $20000 \leq \text{Re} \leq 60000$ at particle volume ratios of $0.00 \leq \phi \leq 0.04$ in a channel with different rib heights. They reported that heat transfer improved as the Re and ϕ increased, and an increment in pressure drop was also observed. Sriromreun et al. [24] experimentally and numerically analyzed the effects of Z-type baffle turbulators on thermal performance in a rectangular duct and indicated that the presence of Z-baffles has an important potential on thermal performance when compared to straight channels. Turgut and Kızılırmak [25] theoretically studied the thermal and flow properties of baffles with different angles ($30^\circ \leq \alpha \leq 150^\circ$) in a channel with a constant heat flux for turbulent flow. They declared that the maximum thermal improvement was found at $\alpha = 150^\circ$ baffle angle. Promvong et al. [26] stated in their experimental studies that Nu increased by about 92-208% compared to straight channels, and the pressure loss rose by 1.76-6.37 times in a channel using inclined horseshoe baffles. Kumar et al. [27] examined the thermal improvement of multiple V-type baffles in the solar air duct. Sahel et al. [28] declared in a numerical study that baffles in a rectangular duct enhanced heat transfer by 65%.

Fluids such as ethylene glycol, propylene glycol, water, and oil, commonly used in engineering fields, have low thermal features. To improve the thermophysical properties of such traditional liquids, nano-sized particles with high thermal conductivity are added. More than one method is used together to obtain a higher heat transfer coefficient. Some works were examined nanofluids with passive methods [29-32]. Heshmati et al. [33] studied the thermal performance of Al_2O_3 , CuO , ZnO and SiO_2 nanofluids at particle volume ratios of $0.00 \leq \phi \leq 0.04$, in the range of $50 \leq \text{Re} \leq 400$ on a backward step with corrugated baffles in different geometries. As a result, it was shown that nanofluids with high particle volume fractions provided high heat transfer rate. They also reported that the inclined baffles have the highest average Nusselt number with high pressure drop. Alnak [34] analyzed the thermal enhancement and friction factor of rectangular baffles with different angles in corrugated triangular channels for the k - ϵ turbulence model. As a result of the study, the results showed that for $\text{Re} = 6000$, the Nusselt number at 90° baffle angle is 52.8% higher than at 60° baffle angle. Ajeel et al. [35] carried out a theoretic work investigating the hydraulic and thermal

performance of ZnO -water nanofluid in a curved corrugated duct with L-shaped baffles for turbulent flow and analyzed the thermohydraulic performance for different Reynolds numbers, baffle angles, blocking rates, and nanoparticle volume ratios for constant temperature conditions. They reported that the baffles caused the thermal enhancement by increasing the eddy formation in the flow. Menni et al. [36] examined the effects of different angles of baffles and nanofluids on hydraulic and thermal enhancement in a heat exchanger for turbulent flow. They declared that the maximum thermal enhancement was found with high Reynolds number and vertical baffles.

In the literature, there are many studies examining thermal and hydraulic behaviours in ducts with different baffle configurations. However, due to the many parameters, new studies continue to find the optimum parameters. The fact that the investigated parameters such as channel and baffle shapes, baffle angles, flow and fluid parameters, nanofluid parameters are quite large, expanded the research to find the best parameters. The main purpose in these studies is to achieve the parameters that ensuring the highest heat transfer with the least pressure drop. In the literature, no definite parameter has been reported that provides the highest thermal enhancement with the lowest friction factor. Therefore, new studies are needed. To date, the effect of baffles angles on the flow of CuO -water nanofluid at varying particle volume ratios in a circular duct has not been investigated. In present study, the flow and thermal enhancement of CuO -water nanofluid at different particle volume fractions ($1\% \leq \phi \leq 3\%$) in a circular duct with different baffle angles ($30^\circ \leq \alpha \leq 150^\circ$) for $200 \leq \text{Re} \leq 1000$ are theoretically analyzed.

2. Material and Method

2.1 Schematic of the Numerical Model

Figure 1 indicates the schematic of the numerical model used in this study. The diameter of the circular duct (D) is 19 mm. At the duct entrance and exit, there is an unheated straight part $L_1 = 0.4$ m ($= 21 D$). The length of the channel consisting of baffles is $L_2 = 0.635$ m ($= 33 D$). The distance between the two baffles is considered as $S = 2D$. The length of the baffles (H) is $0.5D$ and the thickness of the baffles (t) is 0.5 mm. The baffles are placed on the walls of the duct with three different angles (α : 30° , 90° and 150°). The working fluid is the CuO -water nanofluid. Three different particle volume fractions are considered (ϕ : 1%, 2% and 3%). The diameters of the nanoparticles used in the study are considered $d = 20$ -50 nm. The solutions are performed for $200 \leq \text{Re} \leq 1000$ under laminar flow conditions.

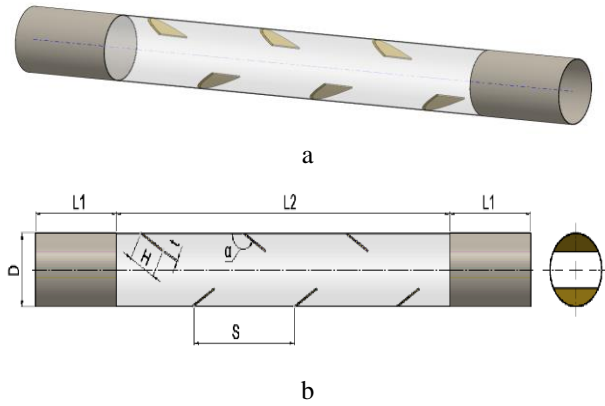


Figure 1. Geometry of the numerical model, a-3d solid model, b-2d scheme

2.2 Numerical Study

In the channel, the nanofluid flows in two-dimensional, laminar and steady conditions. The fluid is Newtonian type, single-phase and incompressible. Body forces and heat transfer by radiation are ignored. According to these assumptions, the governing equations are given by Equations (1) - (3) [37].

$$\nabla(\rho u) = 0 \quad (1)$$

$$\frac{\partial(u_i u_j)}{\partial x_i} = -\frac{\partial P}{\partial x_i} + \frac{1}{\text{Re}} \nabla^2 u_j \quad (2)$$

$$u_i \frac{\partial T}{\partial x_i} = \frac{1}{\text{RePr}} \nabla^2 T \quad (3)$$

The parameters used in the study were determined as Reynolds number (Re), Nusselt number (Nu), thermal enhancement factor (η), friction coefficient (f), and performance evaluation criterion (PEC). The equations for the relevant parameters are presented below.

The Reynolds number (Re) is calculated by Equation (4).

$$\text{Re} = \frac{\rho u D}{\mu} \quad (4)$$

The local Nusselt number (Nu_x) (Eq. 5) and the average Nusselt number (Nu) (Eq. 6) are described as follows [14]:

$$\text{Nu}_x = \frac{q'' D}{k_f (\bar{T}_{w,x} - \bar{T}_{b,x})} \quad (5)$$

$$\text{Nu} = \frac{1}{L} \int_0^L \text{Nu}_x dx \quad (6)$$

Here, q'' is the heat flux, k_f is the thermal conductivity of the fluid, D is the duct diameter, L is the duct length. T_w is the wall temperature of the duct and T_b is the film temperature of the fluid.

The film temperature of the fluid, T_b is computed by Equation (7).

$$T_b = \frac{(T_{in} + T_{out})}{2} \quad (7)$$

The thermal enhancement factor (η) calculated depending on the Nusselt number is defined by Equation (8) [14].

$$\eta = \frac{\text{Nu}_b}{\text{Nu}_s} \quad (8)$$

Here, Nu_b is Nu for the nanofluid in the channel with baffles, and Nu_s is the Nu for the base fluid in the channel with baffles.

The friction factor (f) is found by Equation (9) [14].

$$f = \frac{\Delta P D}{0.5 \rho u^2 L} \quad (9)$$

Here, ΔP denotes the pressure difference between the inlet and outlet of the duct.

The relative friction factor (r) calculated depending on the friction factor is obtained by Equation (10) [14]:

$$r = \frac{f_b}{f_s} \quad (10)$$

Here, f_b is friction factor calculated for the nanofluid in the channel with baffles, and f_s is the friction factor for the basic fluid in the channel with baffles.

The ratio of thermal enhancement to the relative friction factor is defined as the performance evaluation criterion (PEC) and is represented by Equation (11) [4, 14].

$$\text{PEC} = \frac{(\text{Nu}_b/\text{Nu}_s)}{(f_b/f_s)^{1/3}} \quad (11)$$

The numerical model and mesh structure were created by the Gambit software and the element structure of the numerical model with different baffle angles is presented in Figure 2.

Numerical solutions were performed with FLUENT 15.0 [38] solver and iterations were solved with SIMPLE (Semi-Implicit Method for Pressure-Linked Equations) algorithm. A second-order upwind scheme was used to discretize the convection and diffusion terms. The convergence criterion was set as 10^{-6} for all equations. No problem was observed during the calculations for the accepted convergence criterion.

To determine that the solutions are not affected by the number of elements, grid independence testing was applied and Nusselt numbers were calculated for different element numbers. The element numbers 104298, 162864, 198974, 235724, and 284168 were applied to the numerical model at $\text{Re}=600$ and $\text{Re}=1000$ for $\alpha = 150^\circ$ and base fluid. As a result of the grid independence testing, 198974 element numbers were adapted to the numerical model. The variation of the Nusselt numbers with the element numbers is shown in Figure 3 at different Reynolds number ($\text{Re}=600$ and $\text{Re}=1000$).

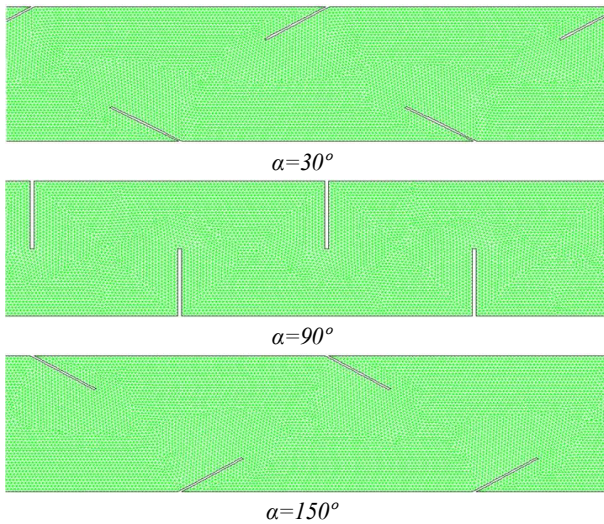
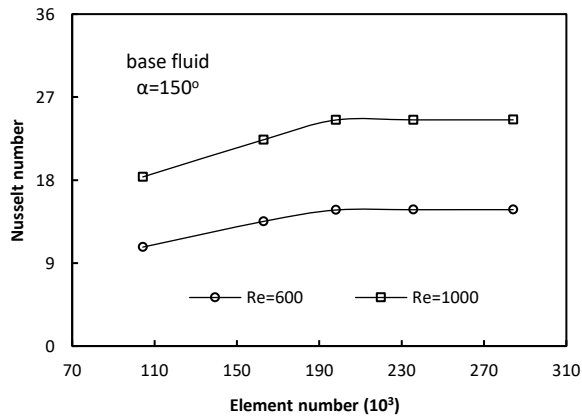


Figure 2. Mesh structures of the numerical model

Figure 3. Variation of Nusselt numbers with element numbers for base fluid at Re=600 and Re=1000 ($\alpha=150^\circ$)

2.3 Thermophysical Properties of Nanofluid

It is assumed that the nanoparticles are homogeneously dispersed in the base fluid. From the thermophysical properties of CuO-water nanofluid, the density was calculated by Equation (12) and the specific heat by Equation (13) [39], the thermal conductivity was calculated by Equation (14) and the viscosity by Equation (15) [40]. The basic fluid is water. Thermo-physical properties of CuO nanoparticle and H₂O are showed in Table 1 [6]. The thermophysical properties were considered constant.

$$\rho_{nf} = (1 - \phi)\rho_{bf} + \phi\rho_{pt} \quad (12)$$

$$C_{nf} = \frac{(1 - \phi)\rho_{bf}C_{bf} + \phi\rho_{pt}C_{pt}}{\rho_{nf}} \quad (13)$$

$$k_{nf} = k_{bf} \frac{[k_{pt} + 2k_{bf} - 2\phi(k_{bf} - k_{pt})]}{[k_{pt} + 2k_{bf} + \phi(k_{bf} - k_{pt})]} \quad (14)$$

$$\mu_{nf} = \mu_{bf}[123\phi^2 + 7.3\phi + 1] \quad (15)$$

Table 1. Thermo-physical properties of CuO nanoparticle and water

	Density [kg/m ³]	Specific heat [J/kgK]	Thermal conductivity [W/mK]	Viscosity [kg/ms]
H ₂ O	998	4182	0.613	0.001003
CuO	6500	533	17.65	-

2.4 Boundary Conditions

The inlet temperature of the nanofluid to the channel is $T_{in} = 293\text{K}$. The “velocity inlet” and “outflow” boundary conditions are used at the entrance and exit of the duct, respectively. The walls of the duct containing the baffles are protected at $T_w = 340\text{K}$. The adiabatic and non-slip boundary conditions are applied for the baffles. The non-slip and adiabatic boundary conditions are defined for the straight sections at the inlet of the duct and the walls of duct consisting baffles.

3. Result and Discussion

The numerical results of the present study were compared to the results of the experimental work realized by Meyer and Abolarin [41]. For this purpose, the heat transfer coefficient, h (W/m²K) were calculated along x/D distances in a straight duct with circular cross section of $D = 19$ mm diameter for $Re = 1331$ and $q'' = 2\text{kW}$ constant heat flux. The results of both studies were given in Figure 4.

In this section, the friction factor and heat transfer of CuO-water nanofluid at different particle volume fractions in a circular cross-section duct in which baffles are placed at different angles are investigated for the range of $200 \leq Re \leq 1000$. To determine the impacts of these parameters on friction factor and thermal performance, the velocity structures, vorticity magnitudes and temperature contours in the duct were obtained.

Figure 5 presents the velocity structures (a), temperature fields (b), and vorticity contours (c) obtained for different Re at $\alpha = 30^\circ$ baffle angle and a constant particle volume fraction ($\phi = 0.03$).

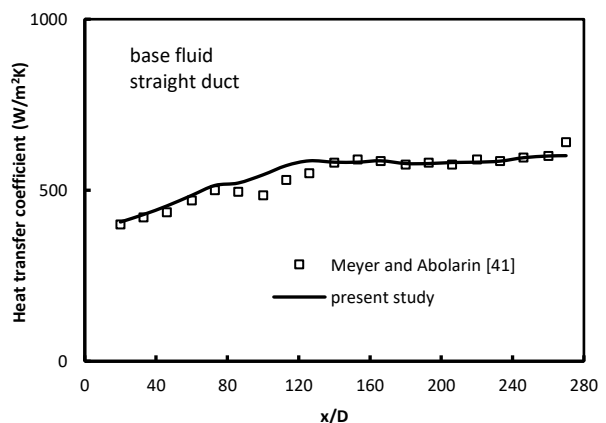


Figure 4. Validity of the numerical solutions (for base fluid)

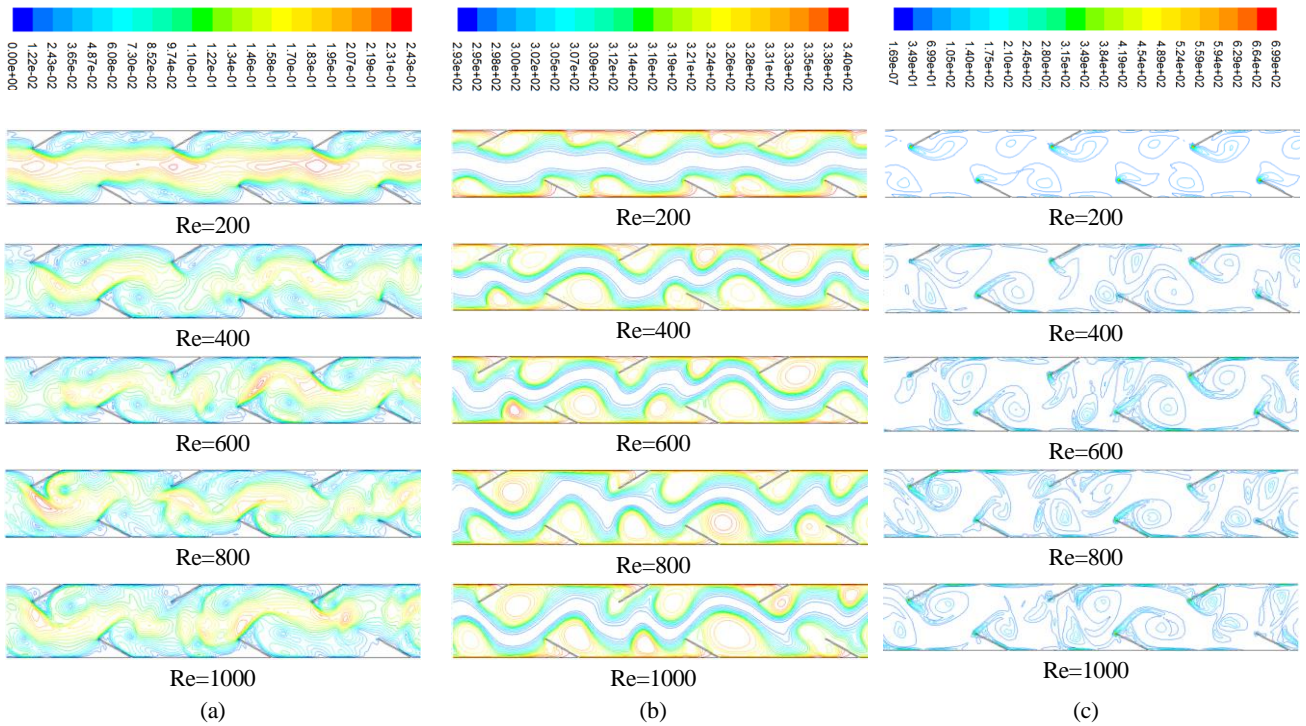


Figure 5. The velocity fields (a), the temperature contours (b), the vorticity magnitudes (c) with different Re at $\phi = 0.03$, $\alpha = 30^\circ$

The velocity fields (Figure 5a) indicate that an oscillation has occurred in the flow due to baffles within the channel. It is seen that the main stream flows as a whole at low Reynolds number, and the separations happen in the flow with the increment in Re. It is indicated that the flow loops occur between each baffle. Increasing the channel inlet velocity causes the flow loops formed in the channel and these structures improve the flow mixing (Figure 5c). Periodic

repetition of this situation after each baffle ensures constant contact of the cold fluid layer in the center of the duct with the warmer fluid layer near the duct walls. Thus, the temperature of the channel surfaces that is in more contact with the cold fluid decreases. With increasing Reynolds numbers, the temperature of the channel surfaces decreased considerably and the heat transfer improved (Figure 5b).

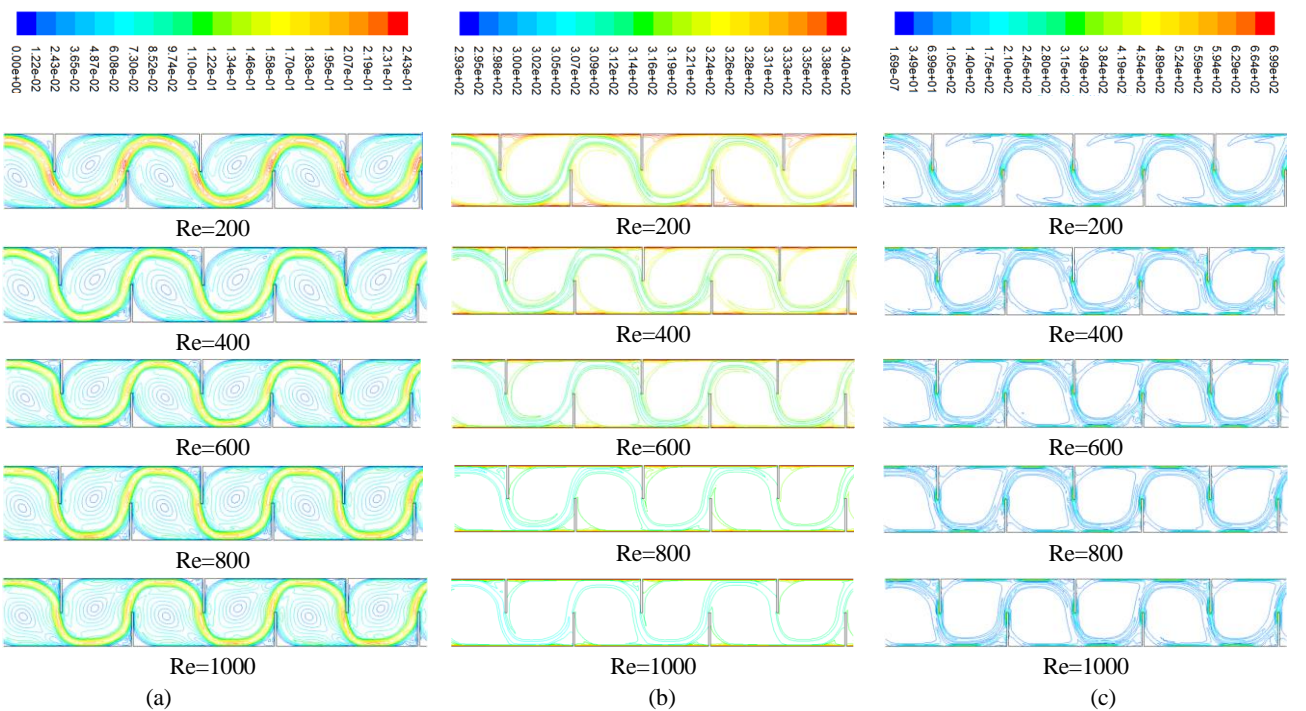


Figure 6. The velocity structures (a), the temperature contours (b), the vorticity fields (c) with different Re at $\phi = 0.03$ and $\alpha = 90^\circ$

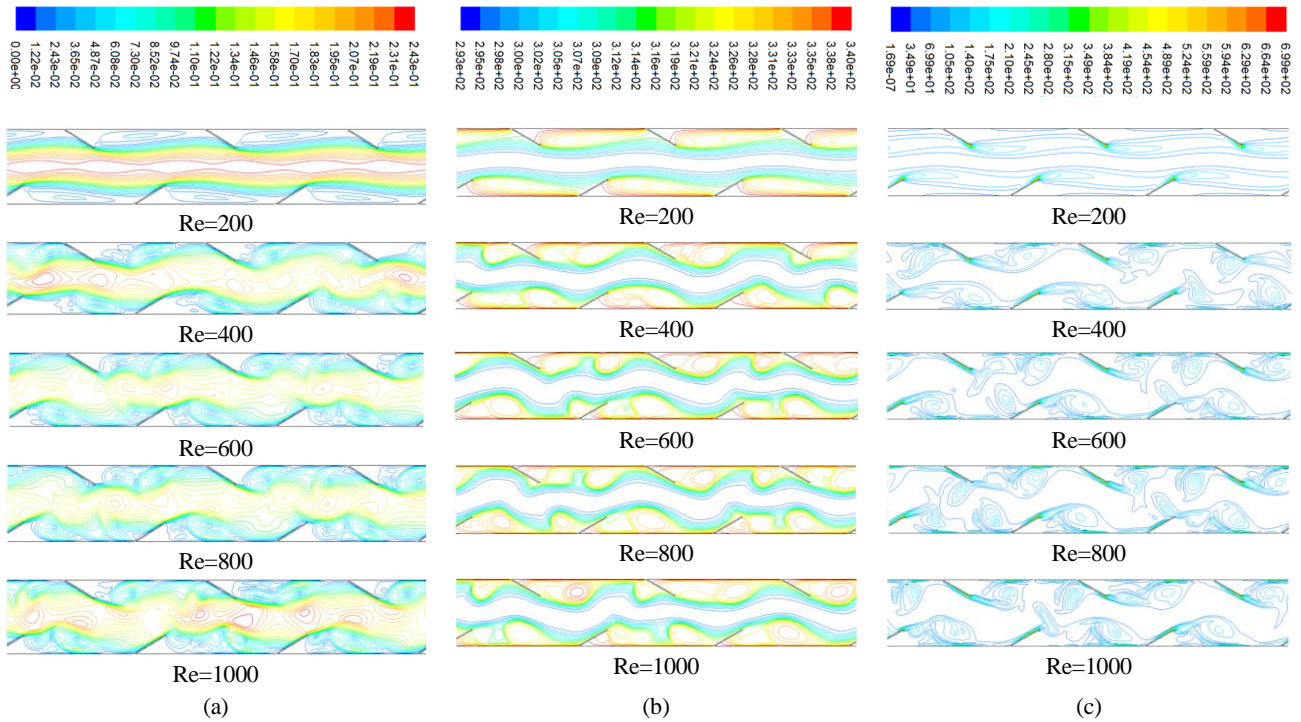


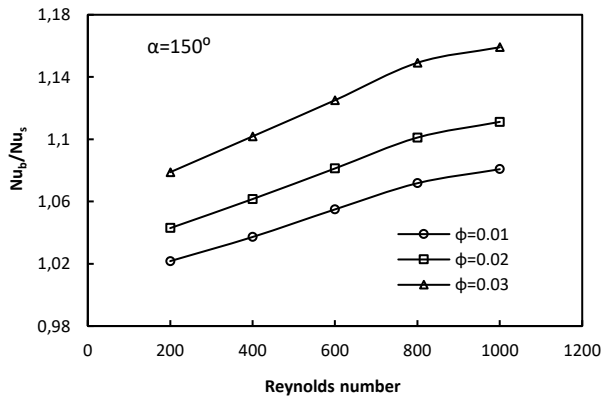
Figure 7. The velocity structures (a), the temperature fields (b), the vorticity contours (c) with different Re at $\phi = 0.03$, $\alpha = 150^\circ$

Figure 6 shows the velocity structures (a), temperature fields (b), and vorticity contours (c) obtained for different Re at $\phi = 0.03$ and $\alpha = 90^\circ$ baffle angle. It is observed that the flow and temperature structures are quite different according to $\alpha = 30^\circ$ baffle angle. The flow structure maintains its integrity in all studied Re. Due to the vertical baffles, the main flow contacts the walls of the duct (Figure 6a). Large recirculation zones are formed between each vertical baffle (Figure 6c). With these cycles, the fluid layer close to the hot channel surfaces is transported to the channel center. Thus, the cold fluid layer replacing the hot fluid layer causes the channel surfaces to cool. The heat transfer rate will increase due to increasing inertia forces and mass flow rate with increasing channel velocity. It is observed that the temperature gradient on the channel surfaces decreases significantly with increasing Re (Figure 6b).

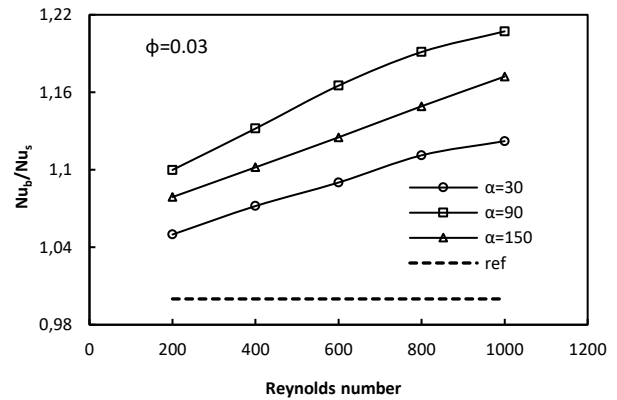
Figure 7 shows the velocity contours (a), temperature fields (b), and vorticity magnitudes (c) obtained for different Re at $\phi = 0.03$ and $\alpha = 150^\circ$ baffle angle. It is seen that the integrity of the main flow structure is not disturbed in all studied Re. The main flow flows as a whole and shows that there are no breaks in the stream. The flow oscillations increase with increasing Re (Figure 7a). It is observed that the flow loops formed longitudinally in the flow direction at low Re, grow transversely between both baffles at high Re and become concentrated all over the channel (Figure 7c). The deterioration of the velocity and thermal boundary layers formed on the channel surfaces due to the baffles diminish the thermal resistance and thus heat transfer is improved. As with other baffle angles,

increasing Re at $\alpha = 150^\circ$ baffle angle increases the heat transfer by decreasing the surface temperature (Figure 7b).

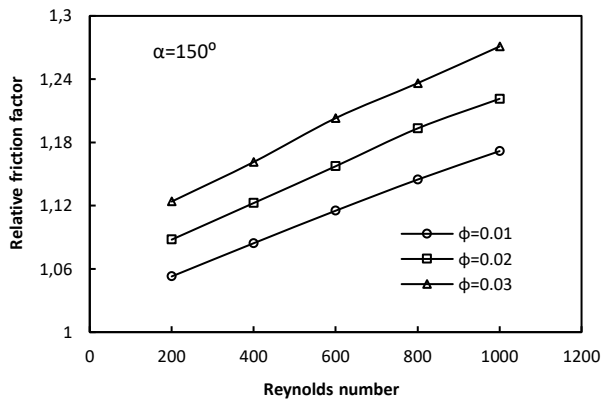
Figure 8 shows the variation of thermal enhancement factor, η (a), relative friction factor, r (b), and performance evaluation criterion (PEC) (c) with Re at different particle volume fractions for $\alpha = 150^\circ$ baffle angle. Thermal enhancement factor increases with increasing the ϕ and Re. It was observed that thermal enhancement factor increased faster in the range of $200 \leq Re \leq 800$ for all tested ϕ , and increased more slowly after $Re \geq 800$. Because the Nu_s value also increases at high Re ($Re \geq 800$). The highest thermal enhancement factor for $\alpha = 150^\circ$ baffle angle was obtained to be about 1.16 at $Re = 1000$ and $\phi = 0.03$. At $Re = 1000$, the thermal enhancement factors for $\phi = 0.02$ and $\phi = 0.01$, were found to be approximately 1.11 and 1.08 respectively (Figure 8a). The relative friction factor increases with increasing ϕ and Re. Pressure loss increases due to the fact that the viscosity of the nanofluid is higher than the base fluid. Moreover, the baffles added to the duct surfaces restrict the flow area. This case increases friction loss. The highest relative friction factor for $\alpha = 150^\circ$ baffle angle was obtained as 1.28 at $Re = 1000$ and $\phi = 0.03$. At $\alpha = 150^\circ$ and $Re = 1000$, the relative friction factor for $\phi = 0.02$ and $\phi = 0.01$, were found to be about 1.22 and 1.17, respectively (Figure 8b). The PEC increases with increasing Re and ϕ . A slight peak occurred at $Re = 800$ for all particle volume fraction. Because after $Re = 800$, the thermal enhancement factor increases more slowly and the friction factor increases more.



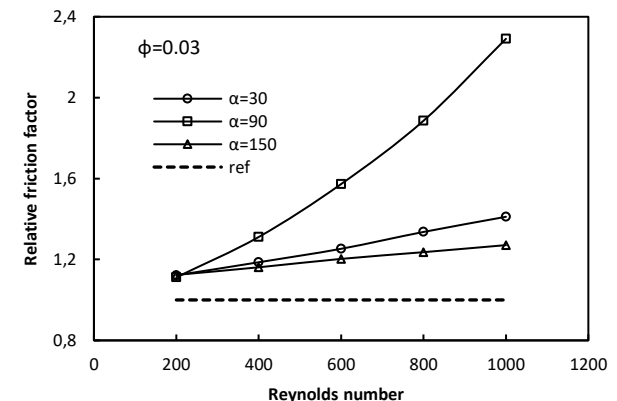
(a)



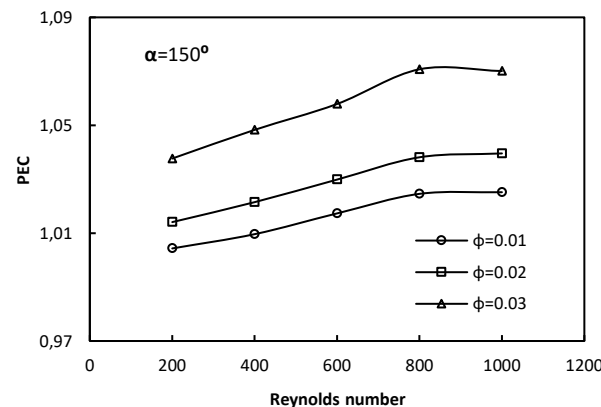
(a)



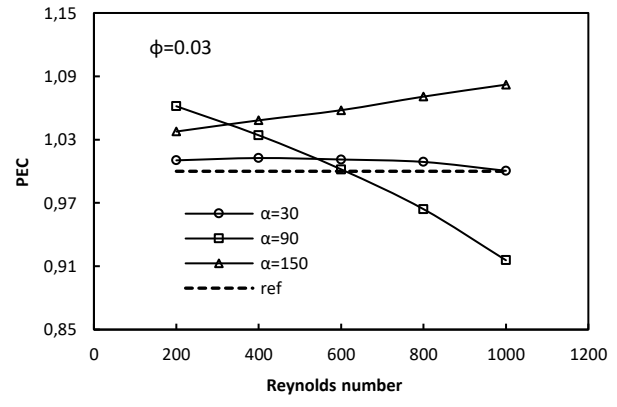
(b)



(b)



(c)



(c)

Figure 8. Thermal enhancement factor (a), relative friction factor (b), and PEC (c) with Re and different particle volume fractions at $\alpha = 150^\circ$

Figure 9. Thermal enhancement factor (a), relative friction factor (b), and PEC (c) with Re and different baffle angles at $\phi = 0.03$.

The highest PEC for $\alpha = 150^\circ$ baffle angle was found to be 1.07 at $Re = 800$ and $\phi = 0.03$. At $\alpha = 150^\circ$ and $Re = 1000$, the PEC for $\phi = 0.02$ and $\phi = 0.01$, were acquired to be about 1.04 and 1.00, respectively (Figure 8c). Due to the nanosized particles added to the basic fluid and the baffles added to the channel surface, significant improvement in heat transfer is achieved, but an acceptable increase in surface friction is also observed.

Figure 9 shows the variation of thermal enhancement factor (a), relative friction factor (b), and PEC (c) with Reynolds numbers at different baffle angles for $\phi = 0.03$.

The dashed straight line represents the base fluid flow in the duct with baffles at the same geometry and is taken as a reference. Thermal enhancement increases with increasing Re. The highest thermal enhancement factor occurs at $\alpha = 90^\circ$ baffle angle, followed by $\alpha = 150^\circ$ and $\alpha = 30^\circ$ baffle angles. The highest thermal enhancement was found to be 1.21 at $Re = 1000$ and $\phi = 0.03$ for $\alpha = 90^\circ$. At $Re = 1000$, the thermal enhancement for $\alpha = 30^\circ$ and $\alpha = 150^\circ$ were found to be about 1.16 and 1.12, respectively (Figure 9a). The relative friction factor increases with increasing Re. It is seen that the lowest friction factor is obtained at $\alpha = 150^\circ$ baffle angle, followed by $\alpha = 30^\circ$ and $\alpha = 90^\circ$ baffle angles. Relative friction factor increases dramatically with increasing Re at $\alpha = 90^\circ$ baffle

angle compared to other angles. This is because vertical baffles highly restrict the flow area. The highest relative friction factor was found to be 2.29 at $Re = 1000$ and $\phi = 0.03$ for $\alpha = 90^\circ$. At $\phi = 0.03$ and $Re = 1000$, the relative friction factor for $\alpha = 30^\circ$ and $\alpha = 150^\circ$ were obtained to be about 1.41 and 1.27, respectively (Figure 9b). The PEC variation differs in all three baffle angles for $\phi = 0.03$. The PEC values were obtained close to the reference value in all studied Re at $\alpha = 30^\circ$ baffle angle. At $\alpha = 150^\circ$ baffle angle, the PEC increases with increasing Re . The reason for this is that the relative friction factor increases less at $\alpha = 150^\circ$ baffle angle than at other angles. At $\alpha = 90^\circ$ baffle angle, the PEC values decrease dramatically with increasing Re . The reason for this is that the relative friction factor increases more than the thermal enhancement at the $\alpha = 90^\circ$ baffle angle. The best PEC was acquired to be about 1.08 at $Re = 1000$ and $\phi = 0.03$ for $\alpha = 150^\circ$ (Figure 9c).

This study summarizes that due to nanoparticles added to the base fluid and baffles added to the duct surface, significant improvement in heat transfer is achieved, but an acceptable increase in friction factor is observed.

4. Conclusions

In present study, the flow and thermal improvement of CuO-water nanofluid were numerically investigated for different particle volume fractions in a circular duct in which baffles were placed at different angles. The effects of baffle angles, particle volume fractions and Re on friction factor and thermal enhancement factor were examined. The velocity structures, vorticity contours and temperature fields were obtained for different parameters in the duct. In numerical simulations, it has been observed that the flow structure and temperature contours were significantly affected by the baffle angles and Re . It was determined that nanoparticle volume fractions and baffle angles have a significant potential in heat transfer improvement according to laminar flow regime. The findings indicated that the thermal enhancement factor increased considerably with a slight friction factor with increasing Re and ϕ . It was determined that the baffle angles have different effects in terms of friction factor and heat transfer. The highest thermal enhancement factor and relative friction factor were obtained at $\alpha = 90^\circ$ baffle angle. The best performance evaluation criteria value was acquired at $\alpha = 150^\circ$. This study shows that baffles inserted into duct have an important potential to improve heat transfer under nanofluid flow if an appropriate baffle angle is used.

Declaration

The authors declared no potential conflicts of interest with respect to the research, authorship, and/or publication of this article. The authors also declared that this article is original, was prepared in accordance with international publication and research ethics, and ethical committee

permission or any special permission is not required.

Author Contributions

S. Akçay studied on methodology, analysis, verification, writing and review of the manuscript. U. Akdag supervised, reviewed and edited the study.

Nomenclature

C	: Specific heat [J/kgK]
D	: Duct diameter [m]
H	: Baffle length [m]
k	: Thermal conduction [W/mK]
L_1	: Unheated channel length [m]
L_2	: Baffled channel length [m]
Nu	: Nusselt number [$Nu = hL/k$]
P	: Pressure [Pa]
Pr	: Prandtl number [$Pr = \mu C_p/k$]
r	: Relative friction factor [$r = f_b/f_s$]
Re	: Reynolds number [$Re = uD/\nu$]
S	: Distance between baffles [m]
t	: Thickness of the baffles [m]
T_{in}	: Inlet temperature of fluid [K]
T_{out}	: Outlet temperature of fluid [K]
T_w	: Surface temperature of the duct [K]
u, v	: Velocity components [m/s]
η	: Thermal enhancement factor [$\eta = Nu_b/Nu_s$]
μ	: Dynamic viscosity [Pas]
ρ	: Fluid density [kg/m^3]
ν	: Kinematic viscosity [m^2/s]
ϕ	: Nanoparticle volume fraction [%]
b	: nanofluid flow in the duct with baffles
bf	: base fluid
nf	: nanofluid
pt	: particle
s	: base fluid flow in the duct with baffles
w	: wall

References

- Menni, Y., A. Azzi, and A. Chamkha, *Enhancement of convective heat transfer in smooth air channels with all-mounted obstacles in the flow path: A review*. Journal of Thermal Analysis and Calorimetry, 2019. **135**: p. 1951-1976.
- Ekiciler, R., M.S.A. Çetinkaya, and K. Arslan, *Effect of shape of nanoparticle on heat transfer and entropy generation of nanofluid-jet impingement cooling*. International Journal of Green Energy, 2020. **17**(10): p. 555-567.
- Husain, S., S.A. Khan, and M.A. Siddiqui, *Wall boiling of Al_2O_3 -water nanofluid: Effect of nanoparticle concentration*. Progress in Nuclear Energy, 2021. **133**: p. 103614.
- Altun, A H., H. Nacak, and E. Canli, *Effects of trapezoidal and twisted trapezoidal tapes on turbulent heat transfer in tubes*. Applied Thermal Engineering, 2022. **211**: p. 118386.
- Akdag, U., S. Akçay, and D. Demiral, *Heat transfer enhancement with laminar pulsating nanofluid flow in a wavy channel*. International Communications in Heat and

- Mass Transfer, 2014. 59: p. 17–23.
6. Arslan, K. and R. Ekiciler, *Effects of SiO₂/water nanofluid flow in a square cross-sectioned curved duct*. European Journal of Engineering and Natural Sciences, 2019. 3(2): p. 101-109.
 7. Akdag, U., S. Akçay, and D. Demiral, *Heat transfer in a triangular wavy channel with CuO-water nanofluids under pulsating flow*. Thermal Science, 2019. 23(1): p. 191-205.
 8. El Habet, M.A., S.A. Ahmed, and M.A. Saleh, *The effect of using staggered and partially tilted perforated baffles on heat transfer and flow characteristics in a rectangular channel*. International Journal of Thermal Sciences, 2022. 174: p. 107422.
 9. Kilic, M., M. Yavuz, and I.H., Yilmaz, *Numerical investigation of combined effect of nanofluids and impinging jets on heated surface*. International Advanced Researches and Engineering Journal, 2018. 2(1): p. 14-19.
 10. Li, Z. and Y. Gao, *Numerical study of turbulent flow and heat transfer in cross corrugated triangular ducts with delta-shaped baffles*. International Journal of Heat and Mass Transfer, 2017. 108: p. 658–670.
 11. Sriromreun, P., *Numerical study on heat transfer enhancement in a rectangular duct with incline shaped baffles*. Chemical Engineering Transactions, 2017. 57: p. 1243–1248.
 12. Mellal, M., R. Benzeguir, D. Sahel, and H. Ameer, *Hydro-thermal shell-side performance evaluation of a shell and tube heat exchanger under different baffle arrangement and orientation*. International Journal of Thermal Sciences, 2017. 121: p. 138-149.
 13. Ekiciler, R. and M.S.A. Çetinkaya, *A comparative heat transfer study between monotype and hybrid nanofluid in a duct with various shapes of ribs*. Thermal Science and Engineering Progress, 2021. 23: p. 100913.
 14. Akçay, S., *Numerical analysis of heat transfer improvement for pulsating flow in a periodic corrugated channel with discrete V-type winglets*. International Communications in Heat and Mass Transfer, 2022. 134: p. 105991.
 15. Ameer, H., *Effect of Corrugated Baffles on the Flow and Thermal Fields in a Channel Heat Exchanger*. Journal of Applied and Computational Mechanics, 2020. 6(2): p. 209-218.
 16. Menni, Y., A. Azzi, and A. Chamkha, *Modeling and analysis of solar air channels with attachments of different shapes*. International Journal of Numerical Methods for Heat & Fluid Flow, 2019. 29(5): p. 1815-1845.
 17. Menni, Y., M. Ghazvini, H. Ameer, M.H. Ahmadi, M. Sharifpur, and M. Sadeghzadeh, *Numerical calculations of the thermal-aerodynamic characteristics in a solar duct with multiple V-baffles*. Engineering Application of Computational Fluid Mechanics, 2020. 14(1): p. 1173–1197.
 18. Salhi, J.E., T. Zarrouk, N. Hmidi, M. Salhi, N. Salhi, and M. Chennaif, *Three-dimensional numerical analysis of the impact of the orientation of partially inclined baffles on the combined mass and heat transfer by a turbulent convective airflow*. International Journal of Energy and Environmental Engineering, Published online 01 June 2022. <https://doi.org/10.1007/s40095-022-00505-5>.
 19. Salhi, J.E., T. Zarrouk, and N. Salhi, *Numerical study of the thermo-energy of a tubular heat exchanger with longitudinal baffles*. Materials Today: Proceedings, 2021. 45: p. 7306–7313.
 20. Nedunchezhiyan, M., R. Karthikeyan, S. Ramalingam, D. Damodaran, J. Ravikumar, S. Sampath, and G. Kaliyaperumal, *Influence of baffles in heat transfer fluid characteristics using CFD evaluation*. International Journal of Ambient Energy, 2022. p. 1–29 <https://doi.org/10.1080/01430750.2022.2063175>.
 21. Razavi, S.E., T. Adibi, and S. Faramarzi, *Impact of inclined and perforated baffles on the laminar thermo-flow behavior in rectangular channels*. SN Applied Sciences, 2020. 2:284, <http://doi.org/10.1007/s42452-020-2078-8>.
 22. El Habet, M.A., S.A. Ahmed, and M.A. Saleh, *Thermal/hydraulic characteristics of a rectangular channel with inline/staggered perforated baffles*. International Communications in Heat Mass Transfer, 2021. 128: p. 105591.
 23. Manca O., S. Nardini, and D. Ricci, *A numerical study of nanofluid forced convection in ribbed channels*. Applied Thermal Engineering, 2012. 37: p. 280-297.
 24. Sriromreun, P., C. Thianpong, and P. Promvong, *Experimental and numerical study on heat transfer enhancement in a channel with Z-shaped baffles*. International Communications in Heat and Mass Transfer, 2012. 39(7): p. 945–952.
 25. Turgut, O. and E. Kızıllırmak, *Effects of Reynolds number, baffle angle, and baffle distance on 3-d turbulent flow and heat transfer in a circular pipe*. Thermal Science, 2015. 19(5): p. 1633-1648.
 26. Promvong, P., S. Tamna, M. Pimsarn, and C. Thianpong, *Thermal characterization in a circular tube fitted with inclined horseshoe baffles*. Applied Thermal Engineering, 2015. 75: p. 1147–1155.
 27. Kumar, R., A. Kumar, R. Chauhan, and M. Sethi, *Heat transfer enhancement in solar air channel with broken multiple V-type baffle*. Case Studies Thermal Engineering, 2016. 8: p. 187–197.
 28. Sahel, D., H. Ameer, R. Benzeguir, and Y. Kamla, *Enhancement of heat transfer in a rectangular channel with perforated baffles*. Applied Thermal Engineering, 2016. 101: p. 156–164.
 29. Jung, S.Y. and H. Park, *Experimental investigation of heat transfer of Al₂O₃ nanofluid in a microchannel heat sink*. International Journal of Heat and Mass Transfer, 2021. 179: p. 121729.
 30. Akdag, U., S. Akçay, and D. Demiral, *Heat transfer enhancement with nanofluids under laminar pulsating flow in a trapezoidal-corrugated channel*. Progress in Computational Fluid Dynamics, An International Journal, 2017. 17(5): p. 302-312.
 31. Akçay, S. *Investigation of thermo-hydraulic performance of nanofluids in a zigzag channel with baffles*. Adiyaman University Engineering Sciences Journal, 2021. 15: p. 525-534.
 32. Akçay, S. *Numerical Analysis of Hydraulic and Thermal Performance of Al₂O₃-Water Nanofluid in a Zigzag Channel with Central Winglets*. Gazi University Journal of Science, 2023. 36(2): in press.
 33. Heshmati, A., H.A. Mohammed, and A.N. Darus, *Mixed convection heat transfer of nanofluids over backward facing step having a slotted baffle*. Applied Mathematics and Computation, 2014. 240: p. 368–386.
 34. Alnak, D.E., *Thermohydraulic performance study of different square baffle angles in cross-corrugated channel*. Journal of Energy Storage, 2020. 28: p. 101295.
 35. Ajeel, R.K., K. Sopian, and R. Zulkifli, *Thermal-hydraulic performance and design parameters in a curved-corrugated*

- channel with L-shaped baffles and nanofluid*. Journal of Energy Storage, 2021. **34**: p. 101996.
36. Menni, Y., A.J. Chamkha, M. Ghazvini, M.H. Ahmadi, H. Ameer, A. Issakhov, and M. Inc, *Enhancement of the turbulent convective heat transfer in channels through the baffling technique and oil/multiwalled carbon nanotube nanofluids*. Numerical Heat Transfer, Part A: Applications, 2021. **79**(4): p. 311-351.
 37. Canli, E., Ates, A. and Bilir, S. Derivation of *dimensionless governing equations for axisymmetric incompressible turbulent flow heat transfer based on standard k- ϵ model*. Afyon Kocatepe University Journal of Science and Engineering, 2020; **20**(6): p. 1096-1111.
 38. ANSYS Fluent user guide & theory guide-Release 15.0, 2015, USA: Fluent Ansys Inc.
 39. Pak, B. and Y.I. Cho, *Hydrodynamic and heat transfer study of dispersed fluids with submicron metallic oxide particles*. Experimental Heat Transfer, 1998. **11**(2): p. 151–170.
 40. Kakac, S. and A. Pramuanjaroenkij, *Review of convective heat transfer enhancement with nanofluids*. International Journal of Heat and Mass Transfer, 2009. **52**: p. 3187–3196.
 41. Meyer, J.P. and S.M. Abolarin, *Heat transfer and pressure drop in the transitional flow regime for a smooth circular tube with twisted tape inserts and a square-edged inlet*. International Journal of Heat and Mass Transfer, 2018. **117**: p. 11-29.